Journal of Sound and Vibration 615 (2025) 119163

Contents lists available at ScienceDirect

Journal of Sound and Vibration

journal homepage: www.elsevier.com/locate/jsvi

Acoustic resonance excitation and source mapping in co-axial piping systems with different junction edge geometries

Atef Mohany [a,*], Omar Hammad [a], Hossam Kishawy [a], Marwan Hassan [b], Mahmoud Shaaban [a,c]

[a] Fluid-Structure Interactions and Noise Control Lab, Ontario Tech University, Ontario, Canada
[b] University of Guelph, Ontario, Canada
[c] Mechanical Engineering Program, School of Engineering and Applied Sciences, Nile University, Giza, 12677, Egypt

ARTICLE INFO

Keywords:
Acoustic resonance
Piping side branches
Strouhal number
Acoustic source modeling
Predictive model

ABSTRACT

In this study, the excitation of acoustic resonance in a coaxial piping system consisting of two opposite pipe branches is experimentally investigated. A lumped element model is used to determine the complex acoustic source, enabling the prediction of resonance excitation under specific flow conditions. The model is validated by assessing the susceptibility of two opposite side branches to acoustic resonance excitation. The predicted acoustic resonance parameters show good agreement with experimental observations in terms of the Strouhal numbers and normalized acoustic pressure amplitudes across a range of flow velocities. Additionally, the effects of rounding and chamfering the edges of the branching junction on resonance excitation are explored. Results indicate that rounded edges produce higher acoustic pressure amplitudes compared to chamfered and sharp edges, with a significant increase in Strouhal numbers at resonance. Furthermore, increasing the rounding radius raises both the onset flow velocity and the lock-in region. The influence of flow development and acoustic radiation losses on the excitation mechanism is also investigated. Findings show that side branches with fully developed flow and reduced acoustic radiation losses to the main pipe are more prone to acoustic resonance excitation and resonate at higher Strouhal numbers. However, the predicted acoustic amplitude reaches a maximum once the upstream distance allows for full flow development over the branching junction.

1. Introduction

In piping systems with closed side branches, flow-excited acoustic resonance where coupling between flow instabilities and acoustic modes materializes can lead to severe structural vibration and fatigue damage, resulting in significant safety and economic consequences [1–5]. As such, investigating the excitation mechanism of acoustic resonances allows for the development of design charts and predictive models to help designers and operators anticipate the onset of resonance and its intensity. Such tools are required to enable the design of systems that mitigate the adverse effects of resonance [6].

To provide an effective model of acoustic resonance excitation in piping systems, a significant body of research aimed to improve the current understanding of the physical acoustic resonance mechanism. In several studies, experimental methods were used to investigate the aeroacoustic resonance excitation under different conditions. Arthurs and Ziada [7] experimentally investigated the aeroacoustic response of an annular duct with closed coaxial side-branches. They showed that annular flow can excite several

* Corresponding author.
E-mail address: atef.mohany@ontariotechu.ca (A. Mohany).

https://doi.org/10.1016/j.jsv.2025.119163
Received 9 October 2024; Received in revised form 23 April 2025; Accepted 27 April 2025
Available online 15 May 2025
0022-460X/© 2025 Published by Elsevier Ltd.

Nomenclature

α	Absorption coefficient
Δp	Dynamic pressure difference across the shear layer
$\mathfrak{I}$	Imaginary component
λ	Wavelength
ω	Angular acoustic frequency
$\mathfrak{R}$	Real component
ρ	Density
a	Speed of sound
c	Edge chamfer
D	Run-pipe diameter
d	Side branch diameter
e	Edge length correction
f_a	Acoustic mode frequency
k	Complex wave number
L	Total run-pipe length
l	Side branch length
l_{up}	Upstream distance from junction to inlet
n	Mode order
p	Acoustic pressure
p^+, p^-	Incident, reflected acoustic wave component amplitudes
p_a	Acoustic pressure amplitude
p_b	Dynamic pressure of the shear layer on the branch side
p_m	Dynamic pressure of the shear layer on the run-pipe side
r	Edge radius
s	Normalized acoustic source
St	Strouhal number
t	Time
U	Upstream flow velocity within the run-pipe
V	Normalized acoustic velocity at the shear layer
v	Acoustic particle velocity
x	Longitudinal side branch coordinate
Z_b	Branch acoustic impedance

acoustic modes. They showed that ratios of the branch length and diameter with respect to the main duct diameter have strong effects on the frequency of the acoustic modes. Okuyama et al. [8] experimentally investigated the case of flow-induced acoustic resonance with multiple side branches. They demonstrated that in the case of coaxial branches, the pressure amplitude increases as the diameters of the main pipe and the branches are increased, unlike single-sided branches. They showed that the two branches strongly couple and form a standing wave with negligible radiation losses. Xiao et al. [9] experimentally investigated the effects of branch length and edge geometry on the acoustic resonance characteristics of closed side branches, showing that chamfered edges may reduce the peak pulsation amplitude of acoustic resonance. A subsequent study by Xiao et al. [10] examined the effect of round and chamfered edges on the acoustic resonance excited by closed side branches. Their results showed that round edges may increase both the resonance strength and the onset flow velocity of excitation, while chamfered edges had no significant effect. In the mentioned studies, resonance was self-excited by the flow. However, investigations were often limited to certain geometries and flow velocities with no generalized method to predict resonance excitation. Shaaban and Mohany [11] showed that acoustic resonance excited by vortex shedding can synchronize sound sources that are otherwise aerodynamically isolated, leading to a substantial increase in sound source. Hanna and Mohany [12] examined the effect of acoustic resonance excitation on the flow over a cylindrical cavity mouth. Their observations suggest that due to the difference in separation time and traveled distances between the cavity edges, the flow over the cavity exhibited strong asymmetry caused by the interference of the recirculation region. This suggests that modifications such as rounding or chamfering to the junction edge between a cylindrical side branch and the main pipe can have a significant effect on the excitation of acoustic resonance.

In addition, several studies used numerical approaches to investigate the coupling mechanism between the acoustic resonance and the flow field. Radavich et al. [13] solved the unsteady, turbulent, and compressible Navier–Stokes equations to model the interaction between the flow and acoustic resonances at low Mach number. Jiang et al. [3] used computational fluid dynamics to model the flow-induced acoustic resonance in closed side branches of a natural gas pipeline. During the excitation process, the

dominant acoustic resonance frequency of the closed side branch is selected and amplified, while other frequency components gradually diminish. However, it requires an extremely fine mesh such that the wall elements are much smaller than typical pipeline length scales, leading to significant calculation costs. Wang et al. [14] carried out fluid dynamics simulations for coaxial rectangular branches with rounded intersection edge, revealing that the rounding radius has a significant effect on the flow fluctuation inside the branches. More recently, Abdelmwgoud et al. [15] showed that opposite shear layers in symmetric configurations are subject to acoustic mode modulation leading to an enhancement of acoustic resonance excitation. Using unsteady compressible simulation of a square cavity, Shaaban et al. [16] showed that the separating turbulent shear layer on the circular edge of a pipe can excite acoustic resonance. They demonstrated that the phasing between the acoustic mode and the flow field is affected by small changes in the geometry, and can lead to changes in both amplitude and orientation of the acoustic mode. Zhang et al. [5] used dynamic delayed detached eddy simulation to explore transient turbulent flow in T-junctions, investigating the effect of the junction geometry ratios on the unsteady flow and flow-induced noise. While numerical simulations are valuable tools to investigate flow-sound interaction at specific flow conditions, the computational requirements become prohibitive for large scale piping networks.

Side branches with no internal flow approach the high-depth limit of the classical flow over deep cavity configuration [17]. When the grazing flow over a cavity mouth suddenly separates at the leading edge, disturbances of the Kelvin–Helmholtz type grow in the free shear layer. A number of these shear layer vortical structures are convected between the leading and trailing edges, depending on both the incident boundary layer thickness and the cavity length. These vortices travel along the shear layer with a convection velocity which depends on the incident flow velocity, the interaction with the cavity mode, and the position along the shear layer [18]. The impingement of the disturbances on the cavity trailing edge produces pressure perturbations that propagates towards the leading edge and organizes the frequency and phase of the separation process, closing a feedback loop which sustains the organized periodic shear layer oscillations [19]. In the fluid-resonant excitation mechanism, the shear layer oscillations over the mouth of a deep cavity may strongly couple with a resonant standing wave mode in the cavity, synchronizing vortex shedding with the acoustic mode particle velocity at the mouth of the cavity [20]. To excite the acoustic mode of a side branch connected to a run-pipe, shear layer oscillations are characterized by sufficiently high frequencies such that the acoustic wavelength is of the same order of magnitude as the length of the side branch. High frequencies require higher flow velocities and therefore an abundant supply of kinetic energy, providing potential for significant oscillation levels. In a side branch, oscillations can only be excited at certain values of wavelength to branch length ratio, selected in a way such that a maximum value of the acoustic pressure amplitude occurs at the closed end of the branch. Deviation from these ideal values occur due to the complex interactions of the flow in the main pipe with the flow inside the branch, including the shear layer perturbation, dynamic mass exchange at the trailing edge, and phase distribution at the end of the branch.

A special case of deep cavities that is of a special interest in many practical applications involves two opposite side branches, such that the two cavities have the same dimensions [13]. Experimental studies observed that the symmetry of the two cavities gives rise to stronger resonance due to the interaction of the compatible frequencies and phases of the two branches [21]. The fluid-resonant mechanism of excitation for this case is shown in figure 1a. The incident flow boundary layer arrives at the two opposite leading edges at similar conditions. Due to the sudden change in the boundary condition, the flow separates into two opposite shear layers that quickly grow into vortical structures. Under favorable conditions, the perturbations in the two shear layers can sustain strong oscillations inside the two opposite side branches. In addition to the typical characteristics for the fluid-resonant mechanism in deep cavities, additional requirements of compatibility within the run-pipe segment should be satisfied to excite different acoustic modes within the two branches. Figure 1b. shows the first five possible configurations of acoustic particle velocity within two opposite branches. If the two branches act as completely independent resonators, exciting the quarter-wavelength mode is possible regardless of the phase between the standing waves. However, a different phase requires a significant transverse pressure gradient within the run-pipe segment. For instance, a phase shift of $\Delta\phi = \pi$ requires the excitation of the fundamental transverse acoustic pressure inside the run-pipe segment, which has a significantly higher natural frequency and therefore is much harder to excite than the branch mode. Moreover, modes that do not have significant acoustic particle velocity at the acoustic source location near the instable shear layer perturbation would not likely engage in the fluid-resonant mechanism. This is the case for the half-wavelength resonator modes within the two side branches regardless of the phase between them. This selection process have been reported in similar cases for the fluid-resonant mechanism where more than a single sound source exists, such as two opposite shallow cavities [15] and vortices downstream of side-by-side cylinders in a transverse resonant mode [11]. For similar configurations, this pressure compatibility requirement resulted in a synchronization of perturbation in the shear layer even if they are not aerodynamically correlated.

To predict the potential for acoustic resonance excitation, several attempts have been made to provide models of the acoustic resonance excitation by simplifying the interactions at the coaxial branch junction. Bruggeman et al. [22] developed a simplified model of the feedback acoustic resonance mechanism through considering the ability of the acoustic perturbation to trigger the formation of coherent vortices near the upstream corner. A minimum level of pulsations in terms of the acoustic particle velocity is required to lead to distinctive vortex formation, which can then be considered by the theory of the vortex sound [23] based on the energy transfer between the fluid and acoustic fields, providing predictions of the lock-on effect observed in deep cavities. A similar approach was used by Dequand et al. [24] to consider the self-sustained oscillations in a closed side branch system by considering the shear layer as a row of discrete vortices convected at constant velocity from the upstream edge towards the downstream edge.

Another category of linear energy-exchange models treat an acoustic source representing the exchanged flow energy as an input to a passive scattering matrix. While such approach is simple in basic piping configurations, it does not account for the coupling between acoustic and flow fields, which is a major source of nonlinearity. Abom et al. [25] developed a model that has the same structure as the traditional multi-port model, but with a scattering matrix that contains information about fluid-acoustic interaction

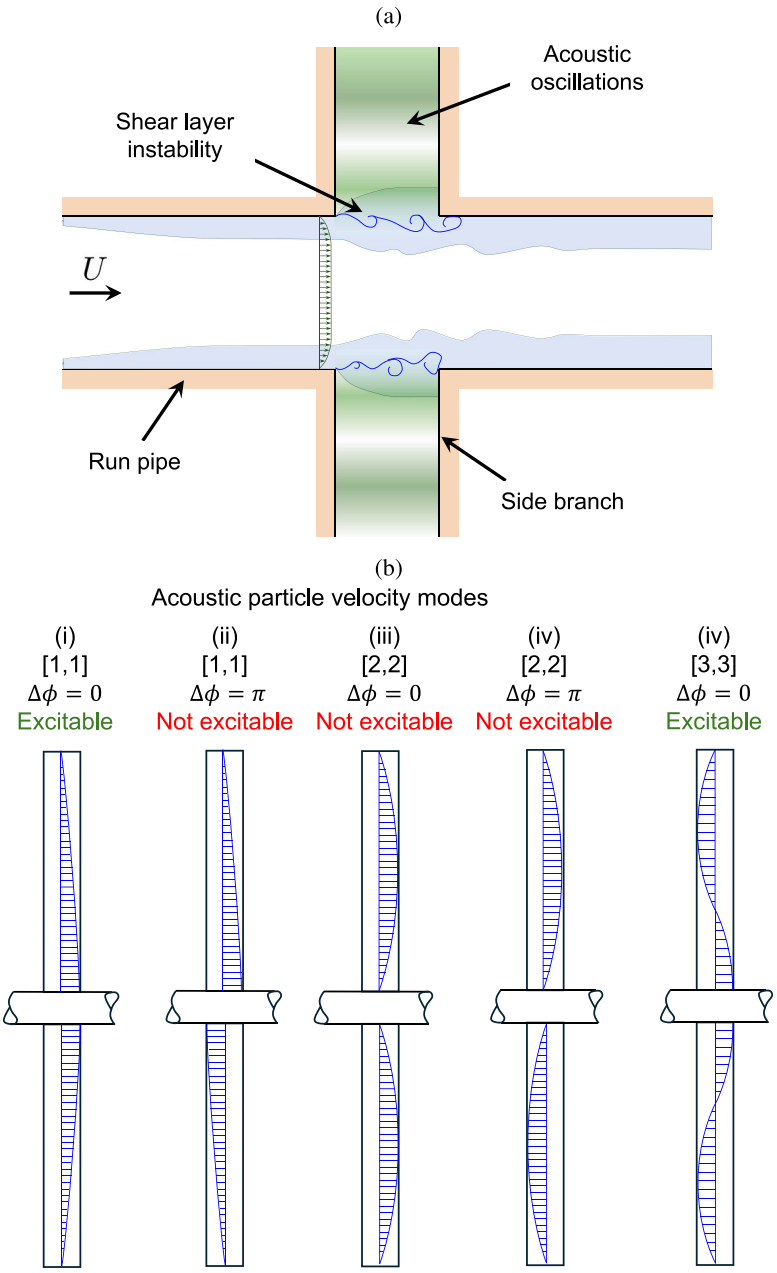


Fig. 1. (a) The fluid-resonant mechanism of excitation in two opposite side branches and (b) the possible acoustic particle velocity states during excitation.

effects, reasonably predicting fluid-excited resonance in whistling cavities. Karlsson and Abom [26] developed a model that includes the effect of flow-acoustic interaction in order to predict self-sustained oscillations using a linear multi-port model.

To mitigate the deficiencies of the linear multi-port method, the use of lumped-element analysis presents an adequate approach to represent the effect of the flow on the aeroacoustic behavior. In this class of models, the energy balance between the flow field and acoustic field is experimentally determined in the form of a lumped source term, including feedback effects and other nonlinear interactions. Bruggeman et al. [27] experimentally characterized the sound source in a single side branch configuration by applying an energy balance between sound production and acoustic dissipation. Kriesels et al. [28] estimated a term representing the acoustic source by balancing the energy produced by the flow and the acoustic impedance of two coaxial side branches by means of a one-dimensional numerical simulation, showing saturation of acoustic pulsations at the condition of acoustic resonance. Meissner [29] provided a model based on theoretical distributed elements with one-dimensional parameters and negligible viscous losses. They showed that the effect of flow to acoustic energy conversion can be compensated for by using a negative impedance term. They noted

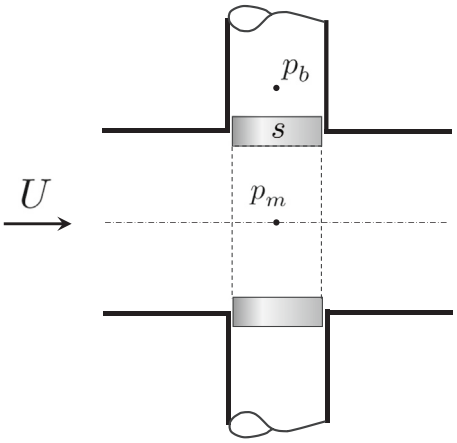


Fig. 2. The lumped impedance model of the shear layer acoustic source.

however that this term is highly nonlinear. Oshkai et al. [30] used detailed acoustic and flow measurements to verify the effect of the accurate geometry representation for the acoustic field modeling on the calculated acoustic power. They used a global quantitative imaging approach to characterize the transformation of the acoustic source structure in terms of patterns of instantaneous and phase-averaged flow velocity, vorticity, and streamline topology as well as time-averaged acoustic power. Valuable insight into the flow behavior near the corners during resonance was obtained albeit with the need of extensive case-dependent measurements. Graf and Ziada [31] experimentally characterized the source impedance in side branch systems attached in coaxial and in tandem exposed to fully developed turbulent flow in the main pipe, which is similar to the geometrical and flow conditions in industrial applications. The source impedance was determined for circular branches. This approach enabled a quantitative evaluation of the non-linear saturation of the shear layer disturbances, providing a method for predicting the acoustic response of coaxial branch systems for different side branch lengths with reasonable accuracy. However, the experimentally determined source maps have been provided only for junctions with sharp edges, and not for rounded edges that are widely used in industrial piping systems.

This work aims to extend the availability of the source mapping to predict acoustic resonance in coaxial side branches with chamfered or rounded connection. The location of the side branches junction in the run-pipe may influence both the acoustic radiation loss and the flow development upstream of the junction. Therefore, it is important to verify whether the location of the coaxial junction has a significant influence on the acoustic resonance and the source model predictions thereof. These objectives are experimentally achieved through an experimental characterization of the aeroacoustic response of coaxial side branches with rounded and chamfered edges in the fully developed turbulent flow conditions expected in industrial piping systems. The acoustic pressure amplitude and the Strouhal numbers are measured for self-excited resonance over a range of flow velocities relevant for industrial applications. Using these measurements, lumped source-term maps are developed to provide predictions of the acoustic pressure, the flow velocity, and the frequency at which resonance is expected. Finally, the effect of the coaxial side branch connection to the run-pipe on the acoustic source is investigated. With this information, the occurrence of acoustic resonance can be anticipated and avoided to ensure safe operation.

2. Methodology

2.1. The shear layer acoustic source model

The excitation of acoustic resonance by shear layer perturbation is modeled based on the experimental identification of an equivalent lumped source term. In this model, the shear layer oscillations represent an acoustic source that acts against the acoustic impedance of the side branch. Acoustic resonance is maintained by the excess of the acoustic power generated by the shear layer over the side branch acoustic dissipation. The excess energy increases the level of acoustic pressure oscillations inside the side branch until a limit cycle is reached. Therefore, estimating the lumped source term at various conditions provides a method to predict the potential of resonance inside the side branches. The following plane-wave assumptions are considered for the acoustic modes within the two opposite side branches. The wavelength of the excited standing wave in the side branch is much larger than the flow structures in the junction such that the acoustic source can be represented by the lumped effect of the shear layer instability. As illustrated in Fig. 2, this effect is modeled as a reciprocating piston that creates a dynamic acoustic pressure difference Δp between the branch p_b and the run-pipe p_m. The dashed line between the pistons denotes the coupling effect of the two shear layers at the mouth of the opposite cavities due to the fluid resonant mechanism.

$$\Delta p = p_b - p_m \tag{1}$$

This lumped effect is represented by a complex source term s, generating acoustic power against the acoustic impedance of the branch. Moreover, it is assumed that acoustic resonance is maintained at a single frequency, neglecting any higher harmonics or

broadband noise effects. During resonance, a steady generation of acoustic power is fully balanced by the visco-thermal dissipation, acoustic radiation, and other losses. The main parameters that control the source term are the junction geometry, the flow velocity, and the acoustic frequency. To estimate the potential pressure level at the closed ends of two opposite side branches at any given frequency and flow velocity, the source term is matched with the acoustic impedance normalized by the flow kinetic energy, such that the values of the Strouhal number $St = f_a d/U$ and acoustic resonance particle velocity can be predicted at steady resonance conditions.

Therefore, maps of the non-dimensional source term s are experimentally constructed to link the acoustic generation of the shear layer to the Strouhal number and acoustic particle velocity at the mouth of the side branches. Following Graf and Ziada [31], the acoustic source term is determined from the dynamic pressure difference at the shear layer as:

$$s = \frac{2\Delta p}{\rho U^2 V} \tag{2}$$

where $\frac{1}{2}\rho U^2$ is the dynamic head in the main pipe and $V = v/U$ is the ratio of the acoustic particle velocity at the branch opening to the flow velocity at the run-pipe. The complex source s acts as a negative impedance, generating acoustic oscillations at the mouth of the side branch to the main system. In complex piping arrangements, the piping network should be solved to identify the eigenvalues of the branches, including the source term s to represent the shear layer contribution to the acoustic response of the system. To determine the Strouhal number and the acoustic particle velocity of the excited resonance, a system of equations representing acoustic flux continuity, consistency of acoustic pressure at the junctions, and the dependency of s on the Strouhal number and acoustic particle velocity is numerically solved. For the configuration of two opposite side branches of equal length, the acoustic pressure at the junction is zero due to symmetry. The acoustic pressure difference across the shear layer can be experimentally determined from the pressure at the two sides through plane-wave decomposition. At any location along the pipe, the plane wave solution can be modeled as the sum of two components traveling in opposite directions:

$$p = p^{+}\exp\left[\mathrm{i}\left(\omega t - k^{+}x\right)\right] + p^{-}\exp\left[\mathrm{i}\left(\omega t + k^{-}x\right)\right] \tag{3}$$

$$v = \frac{p^{+}}{\rho a}\exp\left[\mathrm{i}\left(\omega t - k^{+}x\right)\right] - \frac{p^{-}}{\rho a}\exp\left[\mathrm{i}\left(\omega t + k^{-}x\right)\right] \tag{4}$$

where p and v are the complex pressure and acoustic particle velocity at any location x and time t, p^{+} and p^{-} are the incident and reflected wave amplitudes, $\omega = 2\pi f$ is the angular frequency, $k^{\pm} = \omega/(a \pm U)$ is the wave number. By determining the amplitudes p^{+} and p^{-} in the side branch through two independent measurement of pressure signals at different locations within the branch, the value of p_b can be determined. Likewise, two independent measurements within the run-pipe can provide the decomposed components of the acoustic pressure p_m, providing the source term at the measurement conditions. Extending this process to various flow velocities and edge conditions, maps of source terms can be constructed as outlined in Section 2.3

2.2. The experimental facility

A schematic of the experimental facility is shown in Fig. 3. Experiments were carried out in an open-loop test section driven by a variable-speed screw compressor. The test section is attached to a large box that functions as a flow stabilizer and an acoustically-isolated anechoic enclosure. Flexible hoses are connected to the compressor to isolate vibrations. The compressor outlet is connected to a large acoustic silencer to dampen acoustic oscillations. Air flow at velocities between 10 to 70 m/s is driven into a run-pipe with an inner diameter D of 102 mm. Two opposite side branches with a diameter d of 52.5 mm are connected to the run-pipe. The fundamental acoustic mode of the side branches has a frequency $f_a = 115$ Hz and a wavelength $\lambda = 2.982$ m.

The distance from the junction to the upstream flow inlet is varied from 2.24 m to 6.71 m, equivalent to 0.75λ to 2.25λ to investigate the effect of the inlet conditions on the main pipe fundamental acoustic mode.

The downstream distance from the junction to the flow stabilizer is 5.22 m. This location ensures that the junction is positioned at a pressure antinode within the run-pipe. At a pressure antinode, the run-pipe impedance to the acoustic mode of the side branch is maximum, simulating the practical case of an industrial pipeline that is significantly larger than closed side branches. These conditions ensure that the acoustic radiation into the run-pipe is minimized providing a conservative estimate of the resonance pressure oscillation in the side branch. One end of the side branch is fitted with an adaptable cap allowing for the attachment of an acoustic source to excite acoustic waves at adjustable acoustic particle velocities. The air velocity at the axis of the run-pipe is measured using a pitot tube placed at a distance $10D$ from the flow inlet. The measured flow velocity is corrected using a factor of 0.965 to match the fully-developed flow condition based on the estimate of Doherty et al. [32].

2.3. Shear layer source maps

To determine the complex pressure difference across the shear layer lumped element p, the acoustic pressure is determined from each side of the junction. An external sound source is attached at the closed end of the side branch to impose a plane wave of a single frequency. The flow velocity within the run-pipe is increased between 10 and 70 m/s, to perform measurements at Strouhal numbers between 0.3 and 1.0.

The amplitude of the imposed acoustic pressure by the external source in the side branch is varied to determine the source term required to excite different pressure amplitudes. The acoustic wave is decomposed into a sum of an incident component with

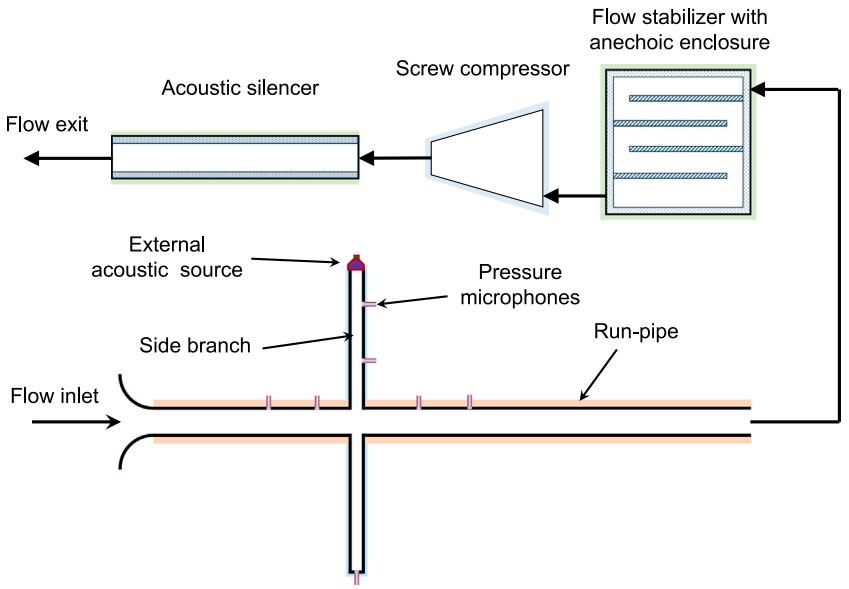


Fig. 3. A schematic of the test setup.

an amplitude p^+ and a reflected component with an amplitude p^- using the two-microphone method [33]. In this method, two independent microphone signals are used to solve for the incidence and reflected amplitudes. Seven PCB model 377A12 pressure microphones are used to measure the acoustic pressure as shown in Fig. 3. On the run-pipe, two microphones are attached upstream and two microphones are attached downstream of the junction to provide an average estimation of the acoustic pressure at the junction from the run-pipe side. Additionally, two microphones are attached on one side of the side branch where the external excitation source is installed, located at $\lambda/8$ from the pressure node of the fundamental acoustic mode to obtain the highest signal-to-noise ratio at the frequency of interest f_a. A microphone attached at the end of the side branch opposite to the excitation source is used to identify the pressure amplitude at the closed end of the opposite side branch. All microphones are flush-mounted to minimize their interference with the fluid flow and connected to a PCB signal conditioner and the amplified signal is measured using an NI data acquisition device at a sampling rate of 5 kHz. All measurements are carried out at relatively low frequencies corresponding to a Helmholtz number less than 0.2 to satisfy the assumption of plane wave propagation. The signals are processed in both the time and complex frequency domains to provide insights into the acoustic characteristics of the system. Once the decomposed pressure components p^+ and p^- are determined, the acoustic particle velocity at any position x inside the duct is calculated from Eq. (4). The procedure described is carried out at flow velocities between 10 to 70 m/s for each configuration to estimate the real and complex components of the source term s at Strouhal numbers between 0.3 and 1.0. Moreover, the source term is provided for different level of acoustic resonance excitation by controlling the imposed acoustic particle velocities between 0.01 to 0.10 of the mean flow velocity. The real and imaginary components of the source term are plotted in maps for determination of the source term at various excitation levels and Strouhal numbers.

Fig. 4 illustrates the use of the source term method to predict the excitation of resonance. The first few acoustic mode frequencies are determined from an eigenvalue analysis. For two opposite side branches of the same length l, the frequency of the acoustic mode of order n is:

$$f_{a,n} = \frac{(2n-1)\,a}{4l}; n = 1, 2, 3, \ldots \tag{5}$$

The real term of the acoustic impedance of the side branch at the frequency f_a is calculated at the conditions of operation using plane wave analysis. The Strouhal number is calculated from the mode frequency f_a, operating flow velocity U, and the cavity mouth characteristic length d. Using the real impedance of the branch and the Strouhal number, the expected normalized acoustic particle velocity v/U can be determined from the source map. On the map, the outer loop is associated with lower Strouhal numbers representing the first shear layer mode, while the inner loop is associated with higher Strouhal numbers, associated with the second shear layer mode. If the matching point lies outside the loop, the system impedance is sufficiently high to suppress resonance excitation (e.g. point (a)). If the matching point lies within one of the loops and has a positive real source component, the corresponding shear layer mode can excite acoustic resonance (e.g. points (b) and (c)). In this case, the acoustic velocity at resonance can be interpolated from the figure. Strouhal numbers to the left side of the graph are not able to excite resonance as the required coupling phase between the shear layer perturbation and the acoustic mode is not possible, as indicated by the negative real impedance value. The maps are presented in this study for different edge configuration and junction locations within the main pipe to provide a tool to predict acoustic resonance excitation under different conditions. Section 3.2 provides an example of the use of the source maps for the case of two side branches with a sharp edge.

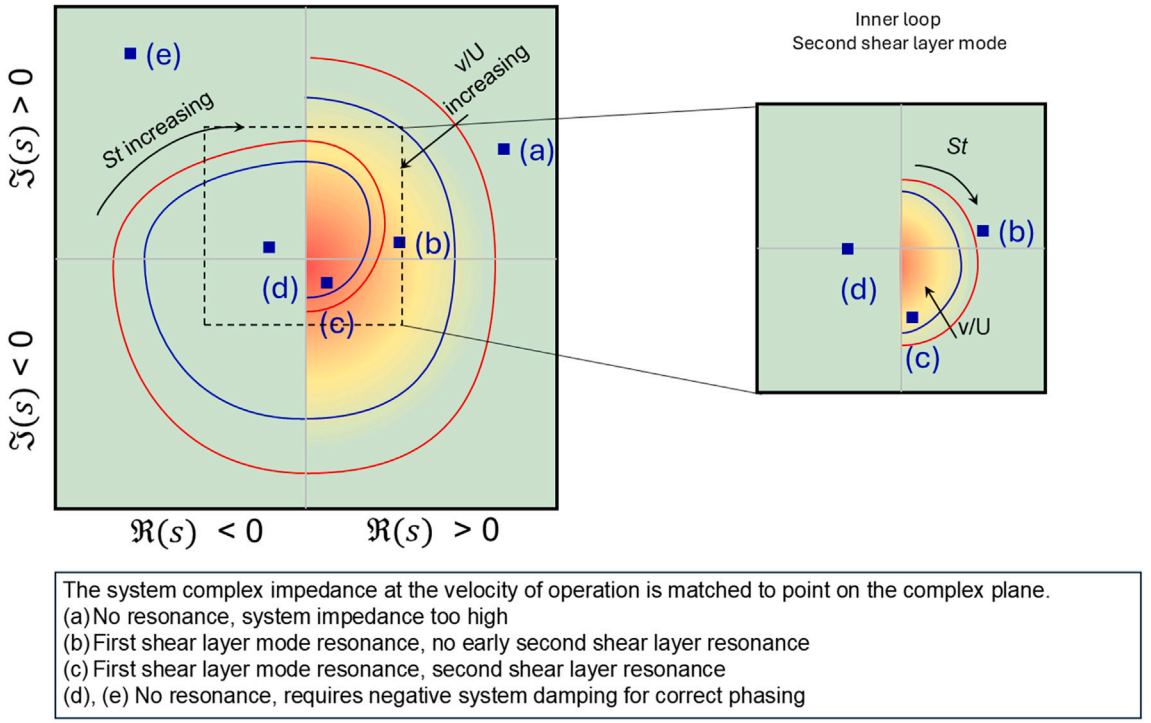


Fig. 4. The use of source term method to predict resonance excitation in coaxial side branches. Green to red contours: increasing v/U. Blue and red lines: different v/U levels. (For interpretation of the references to color in this figure legend, the reader is referred to the web version of this article.)

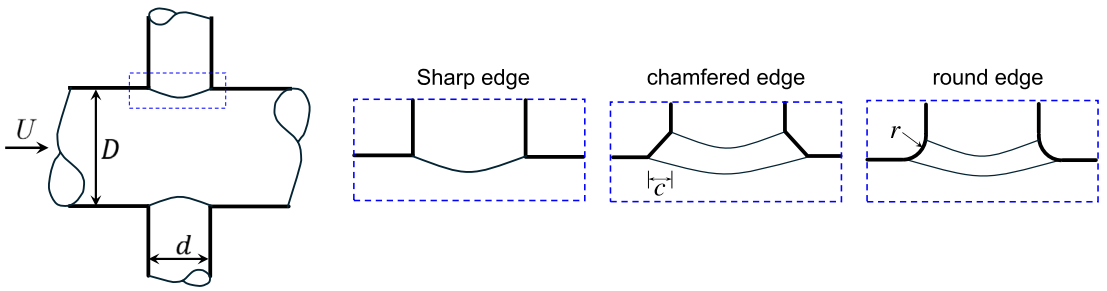


Fig. 5. Left: Side branch junction configuration and source model nomenclature. Right: Edge configurations under consideration.

To investigate the influence of edge geometry at the connection between the main pipe and the coaxial side branch on acoustic resonance excitation, acoustic pressure and frequency were measured at flow velocities up to 70 m/s for coaxial side branches with different edge rounding or chamfering configurations. Four different junction edge rounding radii and four different chamfered edge length are considered as shown in Fig. 5. The considered cases for the round edges have rounding radii of 6 mm, 8 mm, 10 mm, and 12 mm, corresponding to r/d = 0.114, 0.152, 0.190, and 0.228, respectively. Likewise, the considered cases for the chamfered edges have a chamfer edge lengths of 6 mm, 8 mm, 10 mm, and 12 mm, corresponding to c/d = 0.114, 0.152, 0.190, and 0.228, respectively. Ziada and Shine [34] proposes the following Strouhal number definition to account for shear layer rounding:

$$St = \frac{f_a(d+2r)}{U} \quad \text{For rounded edges} \tag{6}$$

$$St = \frac{f_a(d+2c)}{U} \quad \text{For chamfered edges} \tag{7}$$

In Eq. (7), the Strouhal number definition is extended to chamfered edges to verify whether it accurately captures the changes introduced to the aeroacoustic response.

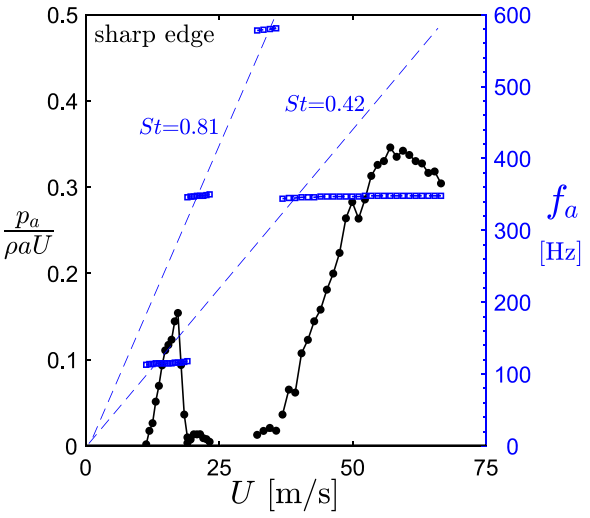


Fig. 6. The amplitude and frequency of the self-excited acoustic resonance over two co-axial side branches with sharp edge.

3. Aeroacoustic behavior of sharp-edged coaxial side branches

3.1. Self-excited acoustic resonance

Fig. 6 shows the self-excited aeroacoustic response of two opposite sharp-edged side branches. The figure shows that a strong acoustic pressure is observed over a wide range of flow velocities over several stages. First, the acoustic pressure starts to increase at 18 m/s. The normalized pressure increases as the flow velocity increases up to a peak value of 0.16 at $U = 20$ m/s. The acoustic pressure decreases rapidly to its background level afterwards. Over this range of flow velocities, the acoustic pressure signal has a frequency equal to the side branch first acoustic mode of $f_a = 115$ Hz. With a slight increase of flow velocity to 22 m/s, a small increase in acoustic pressure can be observed at a frequency of 345 Hz. That frequency corresponds to the third acoustic mode of the side branch, with 1.5λ inside the branch. This mode is excitable by a shear layer over the cavity mouth as it has an acoustic velocity antinode at the location of maximum flow velocity perturbation over the cavity mouth. Due to its higher frequency, this acoustic resonance has higher viscous attenuation losses and the normalized acoustic pressure stays below 0.2. A further increase in flow velocity shows another stage of low acoustic pressure at 30 m/s, correlated with the next excitable acoustic mode of the branch length, which corresponds with $l = 2.5\lambda$. Another increase in the flow velocity yields much higher normalized acoustic pressure, reaching $p/\rho aU = 0.33$ at 60 m/s. The frequency of this acoustic resonance matches the third acoustic mode of the branch, with a branch length of 1.5λ. Notably, Fig. 6 shows that two distinct Strouhal numbers corresponding to the first and second shear layer separation modes are present. These Strouhal numbers are extracted using the frequency and flow conditions at which the acoustic resonance pressure exceeds $p_a = 0.05$ as a threshold for resonance. The two modes, at $St = 0.42$ and $St = 0.81$ coincide with the first three excitable acoustic modes resulting in the observed ranges of acoustic resonance, in agreement with the Strouhal numbers observed by Graf and Ziada [31]. The first shear layer mode excites a stronger resonance than the second shear layer mode.

An interesting feature in Fig. 6 is a slight increase of the acoustic frequency as the flow velocity increases. This increase can be attributed to the interactions of the flow and acoustic fields during the initiation of the lock-in condition. As the two fields engage in the energy exchange mechanism, the phase of the acoustic impedance changes very rapidly. Consequently, a slight increase to the flow velocity reduces the time delay of the shear layer perturbation with respect to the acoustic mode. During resonance, the acoustic feedback mechanism requires that the acoustic mode and shear layer oscillations complete full cycles of oscillation with a fixed phase. With the decrease of the flow perturbation phase delay, keeping the phase-locked condition requires an increased phase delay by the acoustical system, which results in a slight increase of the frequency of the self-sustained oscillation. This mechanism is similar to that observed by Ma et al. [35] in a Helmholtz resonator and by Nagy et al. [36] in a recorder.

3.2. Prediction of acoustic resonance

The source term map for the configuration of two opposite side branches with a sharp edge is shown in Fig. 7. This figure shows the relationship between the Strouhal number St, the aeroacoustic complex sound source term s, and the forced normalized acoustic particle velocity V. The real part of s represents the component of the acoustic power generation that is in phase with the acoustic mode oscillations inside the side branch such that acoustic power is transferred from the shear layer perturbation to the acoustic mode. The imaginary part of s represents the reactive component of the acoustic power which influences the phase and frequency of the resonant acoustic mode in the branch. A change in Strouhal number, driven by a change in the flow velocity at constant excitation frequency, results in a change in the complex source characteristics. At higher values of V, stronger acoustic mode inside

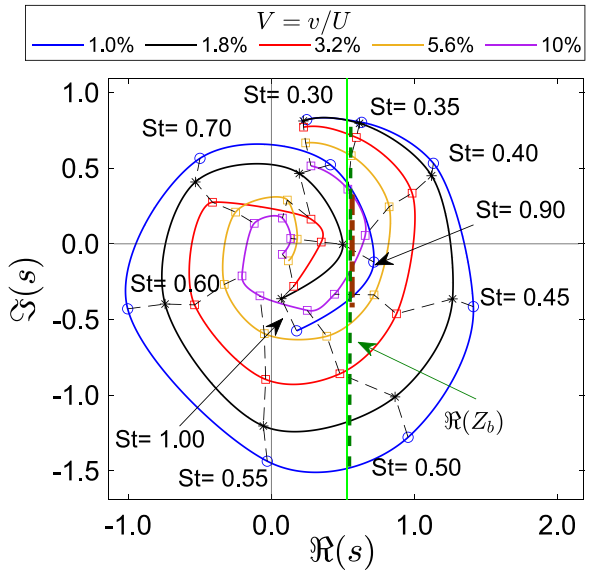


Fig. 7. The complex sound source term s at different normalized acoustic particle velocities ($V = v/U$) for a side branches with a sharp edged junction. Dashed lines (- - - -) and (- - - -) indicate overlap with the superimposed side branch acoustic impedance for the first and second shear layer modes; respectively.

the side branch results in a weaker contribution of the source to the acoustic mode as a result of the increased acoustic losses. In agreement with Graf and Ziada [31], the acoustic source term decreases proportionally with $\sqrt{V}$, such that the acoustic amplitude reaches a limit cycle for each acoustic flow velocity. As the Strouhal number increases, indicating higher shear layer modes with a higher number of smaller vortices between the leading and trailing edges, the source term decreases. Notably, the source term becomes a positive real value, indicating maximum generation in-phase with the acoustic pressure oscillations, at $St = 0.42$ and 0.90, which are the typical values at which the first and second shear layer aerodynamic modes are observed over a cavity.

The points on the map in Fig. 7 can be interpreted as the acoustic real impedance of the side branch where resonance is sustained at the indicated value of the acoustic particle velocity. A coaxial branch with a higher viscous losses, indicated by a higher real component of acoustic impedance at its acoustic mode frequency, would result in a lower acoustic particle velocity and thus less acoustic pressure amplitudes. If the impedance is sufficiently high, such that the normalized branch impedance always falls outside the map region in Fig. 7, resonance is not expected at any flow velocity for that map. A simple procedure can be followed to determine the expected acoustic particle velocity at any flow velocity. The acoustic impedance of the piping system susceptible to excitation is determined at the junction, taking into account the flow velocity. For each side of the coaxial branch, the branch impedance is:

$$z = \frac{\rho a}{\mathrm{i}\tan\left(k(l+e)\right)} \tag{8}$$

where $l+e$ is the end-corrected length of the branch. The real part of the impedance represents the viscous losses. To dimensionally align with the aeroacoustic sound source, one can normalize the impedance term by the flow kinetic energy and the acoustic velocity ratio:

$$Z_b = \frac{Z}{\frac{1}{2}\rho U v} = \frac{2}{\mathrm{i}M\tan(k(l+e))}\left(1 - \frac{\alpha}{k} + \mathrm{i}\frac{\alpha}{k}\right) \tag{9}$$

where α is the air absorption coefficient, calculated according to the model of Tijdeman [37]. The power generated by the lumped element representing the shear layer interaction with the acoustic mode is dissipated in the side branch impedance such that $Z_b = s$. At typical frequencies of piping systems, the frequency is sufficiently low such that the real impedance, representing the viscous dissipation has no dependence on the frequency, while the reactance changes significantly with the frequency. Therefore, coupling between the shear layer source and the branch impedance is expected to take place at a nearly constant value of Z_b, represented by the vertical line $\Re(Z_b) = 0.535$ in Fig. 7. The intersection between the map and the acoustic branch impedance indicates that resonance is likely. Each point over that range is determined such that s is equal to the system impedance Z_b and matched to the source term as illustrated in Fig. 4. By varying the flow velocity, the aeroacoustic response of the system can be determined. The expected acoustic pressure amplitude p_a is calculated at the antinode of the acoustic pressure as:

$$\frac{v}{U} = \frac{p_a}{\rho a U} \tag{10}$$

Fig. 8 compares the model predictions with measured acoustic response for a coaxial branch with sharp edges. The colors of the lines indicate the corresponding region of overlap from Fig. 7. The first shear layer mode overlaps the source map over low Strouhal

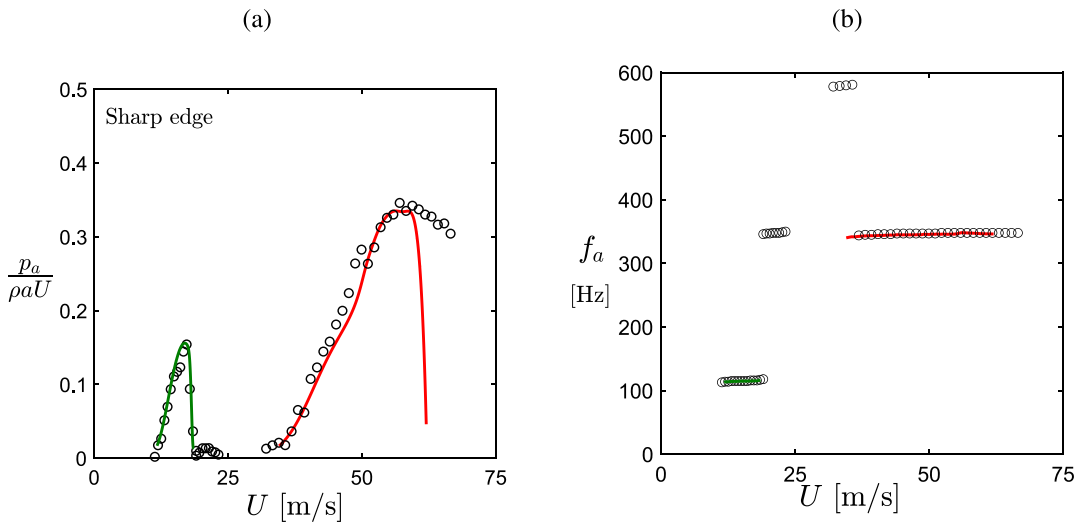


Fig. 8. Comparison of the (a) acoustic pressure amplitude and (b) mode frequency of the excited acoustic resonance for the sharp edge configuration. (○) Measured values, (——) Model predictions for the first shear layer mode, (——) Model predictions for the second shear layer mode.

numbers St between 0.34 and 0.52, as the flow velocity is increased. Meanwhile, the second shear layer mode overlaps over Strouhal numbers St between 0.85 and 0.93. As a result, the flow velocity required for excitation of acoustic modes by the second shear layer mode is lower, which agrees with the observations in Fig. 6 and the model predictions in Fig. 8. The predicted acoustic pressure values and frequencies are in good agreement. However, they capture the excited acoustic resonance when the normalized acoustic pressure exceeds the threshold of 1% set by the outer limit in Fig. 7. The model successfully predicts the initiation of acoustic resonance at $U = 18$ m/s, and the peak acoustic pressure value $p_a/\rho aU = 0.16$ at $U = 20$ m/s. For the excitation of the second acoustic mode by the first shear layer mode at higher flow velocities, the model predicts the acoustic pressure initiation and peak. The model starts to deviate at $U = 60$ m/s as turbulence and background noise start to have a significant effect on the measured acoustic pressure level, deviating from the assumptions of the model. While this warrants further investigation, it is beyond the scope of the current work.

4. Effect of cavity edge geometry on the self-excited acoustic resonance

4.1. Effect of edge rounding

Fig. 9 presents the aeroacoustic response of two opposite side branches with rounded edges. The most notable effect of rounding the junction edges is the significant increase in the acoustic pressure for modes excited by the first shear layer mode. Increased rounding results in a higher normalized acoustic pressure, varying from 0.3 for $r = 6$ mm to 0.4 for $r = 12$ mm, compared with 0.15 for the sharp edged junction. The acoustic resonance strength excited by the first shear layer increases to more than 0.4 for $r = 12$ mm compared with 0.35 for the junction with sharp edges. The Strouhal number is slightly affected by rounding the edge. For the first shear layer mode, it increases from $St = 0.53$ for $r = 6$ mm to $St = 0.58$ for $r = 12$ mm, compared with 0.42 for the junction with a sharp edge. On the other hand, the second shear layer mode fails to excited acoustic resonance. Finally, increasing the rounding radius results in acoustic resonance over a larger range of flow velocities. For $r = 6$ mm, first acoustic mode resonance is observed for a lock-in flow velocity range from $U = 15$ m/s to 25 m/s compared with $U = 16$ m/s to 20 m/s. For $r = 12$ m/s, the lock-in range is higher, from $U = 15$ to 35 m/s. On the other hand, the second acoustic mode is excited nearly at the same flow velocity for all cases.

Fig. 10 shows the acoustic source maps for the same cases with rounded edges in Fig. 9. When compared to the source map for the sharp edge, two notable differences stand out. First, the map is rotated slightly counterclockwise such that the Strouhal numbers on the horizontal axis are higher. This results in increased Strouhal numbers during the peak of resonance. Second, the inner loop of the map which includes Strouhal numbers higher than 0.8 has lower source strength. This implies that the excitation of acoustic modes by the second shear layer mode is more challenging, as observed in the aeroacoustic response of the cases with round edges.

4.2. Effect of edge chamfering

The aeroacoustic response of two opposite side branches with chamfered edges is shown in Fig. 11. The observed acoustic pressure amplitude and frequency indicate that chamfering resulted in a behavior similar to edge rounding over the same range of flow velocity. In addition to exciting the acoustic resonance over the same flow velocity range between $U = 15$ m/s and $U =$

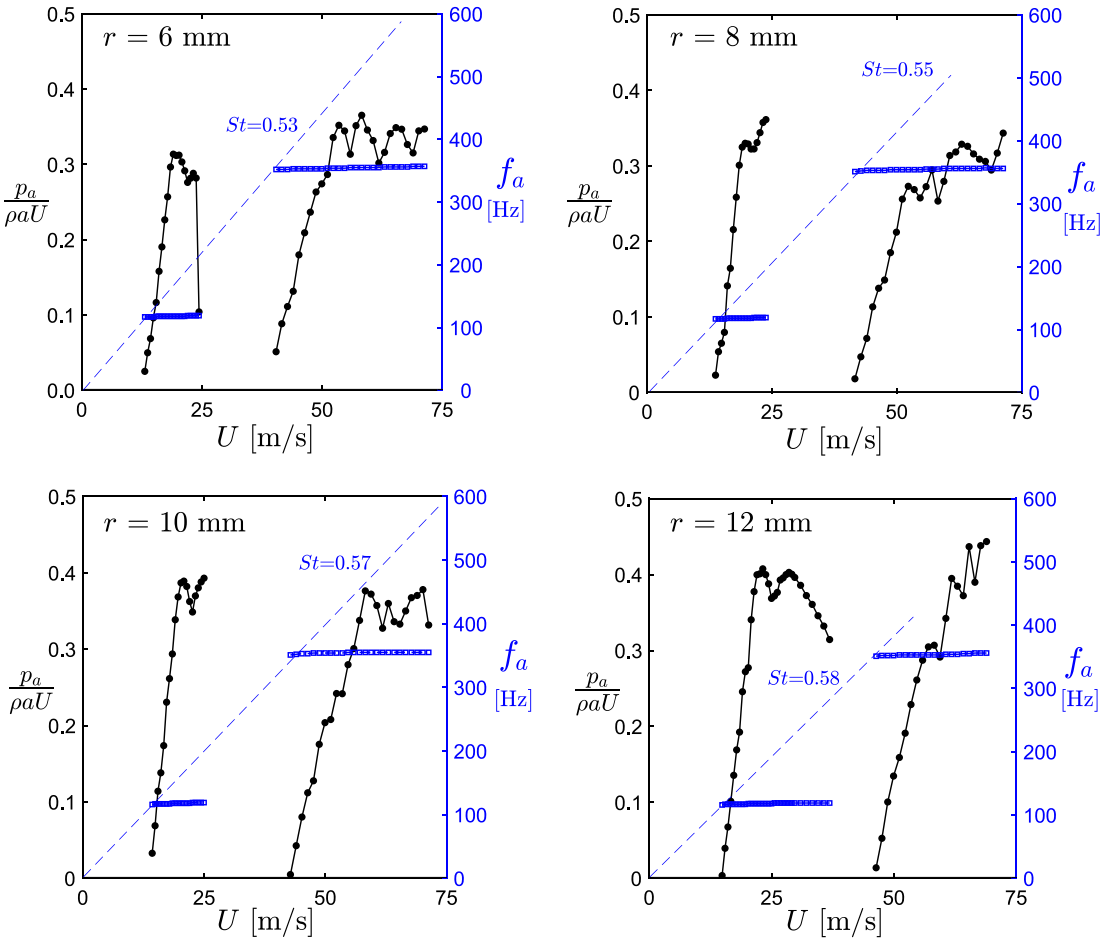


Fig. 9. The aeroacoustic response of coaxial side branches with different rounded edges.

23 m/s, the acoustic pressure of the first acoustic mode excitation by the first shear layer mode reaches a normalized acoustic pressure of 0.3, slightly lower than the rounded case but nearly double the case with the sharp edge. However, the second acoustic mode excitation by the first shear layer mode starts at U = 40 m/s, and reaches a peak of 0.3, lower than the cases with sharp and rounded edges, indicating that the changes from the case of a junction with sharp edge are related to the common features of rounded and chamfered edges. First, the longer shear layer is expected to have a considerable effect on its aerodynamic stability, such that cases with higher radii or chamfered length are more susceptible to perturbation at the same flow velocity. Second, the effect of the edge geometry on the Strouhal number does not seem to be fully captured in Eqs. (6) and (7). As these expressions were initially deduced for aerodynamic fluctuations at the junction, they do not seem to accurately take the effect of the acoustic resonance on the shear layer.

Fig. 12 presents the source maps for the cases with chamfered edges. The patterns in the maps highlight two effects. First, the smaller extent of the inner loops postulates that acoustic mode excitation by the second shear layer mode is expected over a limited range of flow velocities, even for piping branches with low impedance. Second, the same rotational shift results in higher Strouhal numbers during peak excitation of acoustic resonance.

Fig. 13 shows the effect of junction edge geometry on acoustic resonance excitation for the first acoustic mode in comparison with the sharp edge. As the rounding radius r or the chamfer edge length c increase, the Strouhal number of the first shear layer mode increases nearly linearly. The Strouhal numbers are higher for the rounded edge than the chamfered edge. In Fig. 13b, the same trend applies to the acoustic pressure at the peak of resonance. The increase in rounding radius or chamfering edge length results in an increased acoustic pressure. Interestingly, similar observations were reported by Omer et al. [38] for rectangular cavities. Moreover, the normalized flow velocity $U_{onset}/f_a d$, at which resonance is initiated is shown in Fig. 13c. For cases with chamfered edges, resonance started at higher flow velocities, compared with cases that have rounded or sharp edges. The increase in rounded edge radius and chamfered edge length resulted in further increases in the normalized onset flow velocity. Additionally, the range of flow velocities ΔU over which first acoustic mode resonance is observed is shown in Fig. 13d. Cases with rounded edges resulted in resonance over a larger range of flow velocities. Between r/d = 0.12 and 0.20, the lock-in range was nearly constant at $\Delta U/f_a d$

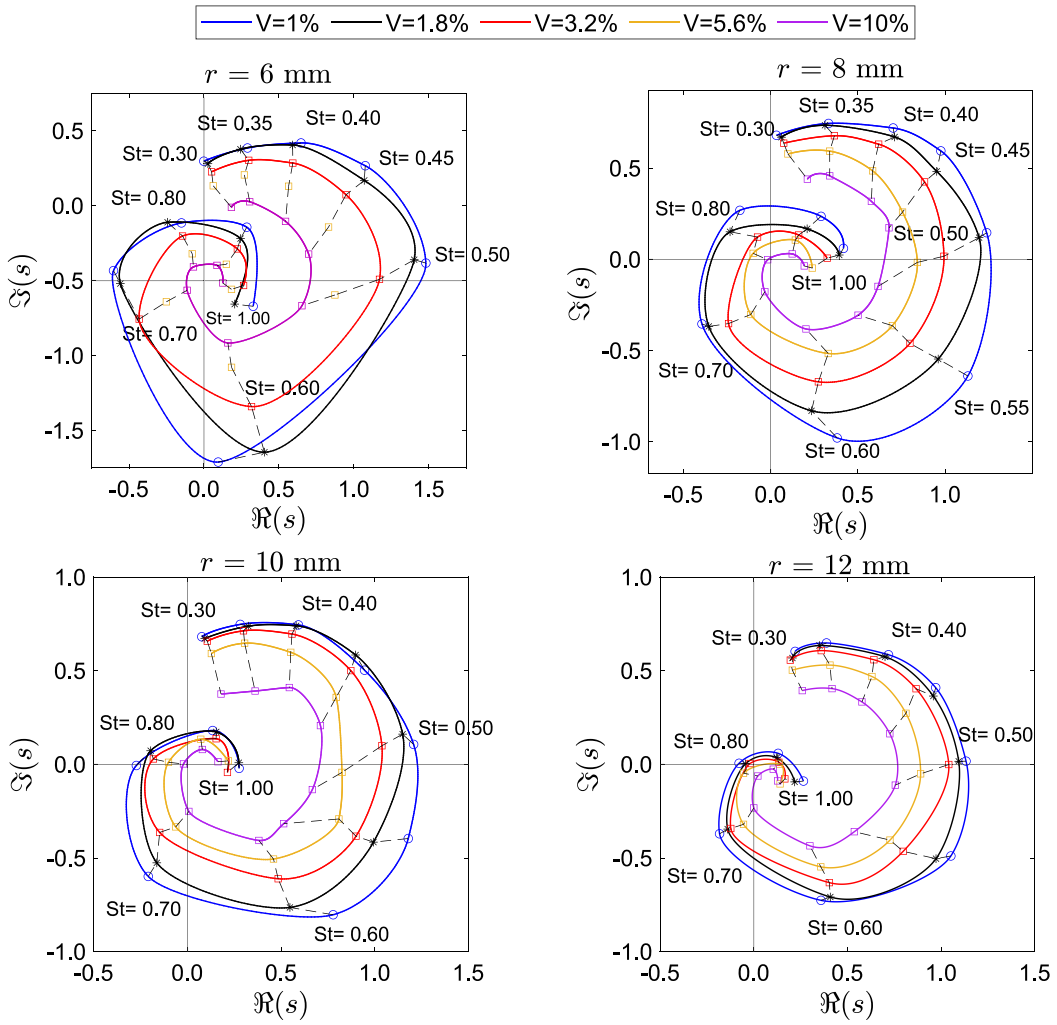


Fig. 10. The aeroacoustic complex sound source for coaxial side branches with different rounded edges.

= 1.8. At $r/d = 0.23$, it increased abruptly to 3.6. Meanwhile, the increase in chamfered edge length resulted in a linear increase in the extent of the lock-in region.

5. Effect of upstream distance from the main pipe inlet

In this section, the influence of the upstream distance on the aeroacoustic resonance of the coaxial side branch and the aeroacoustic sound source is investigated. Increasing the upstream distance moves the open acoustic boundary condition further from the coaxial side branch, thereby reducing reflections from the open end due to acoustic attenuation and viscothermal losses. To ensure that the acoustic mode shape in the main pipe had no effect on shear layer perturbations, the acoustic impedance of the upstream pipe at this frequency is maximized. This is achieved by limiting the upstream pipe length to an odd number of quarter wavelengths of the first excited acoustic mode in the coaxial side branch. Four different junction locations were tested, as shown in Fig. 14 and Table 1. For upstream distances of $3\lambda/4$ and $5\lambda/4$, the flow at the junction is not expected to be fully developed. For the two other cases, with upstream distances corresponding to $7\lambda/4$ and $9\lambda/4$, the flow at the junction is fully developed flow.

Fig. 15 shows that influence of the upstream distance on the complex source term induced by the shear layer. The figure shows that the case with the shortest distance to the upstream end, $l_{up} = 3\lambda/4$, had a lower value of the source term. A lower source term indicates that the acoustic resonance at the same conditions is lower than the other three cases, which highlights the effect of the attenuation losses in the main pipe. Notably, the longer upstream distance had an effect on the Strouhal number. The source maps for longer upstream distances in Fig. 15 are rotates counterclockwise such that the value of St that results in a purely real source increases as the upstream distance increases, indicating that the shear layer perturbation is influenced by distance allowed for the

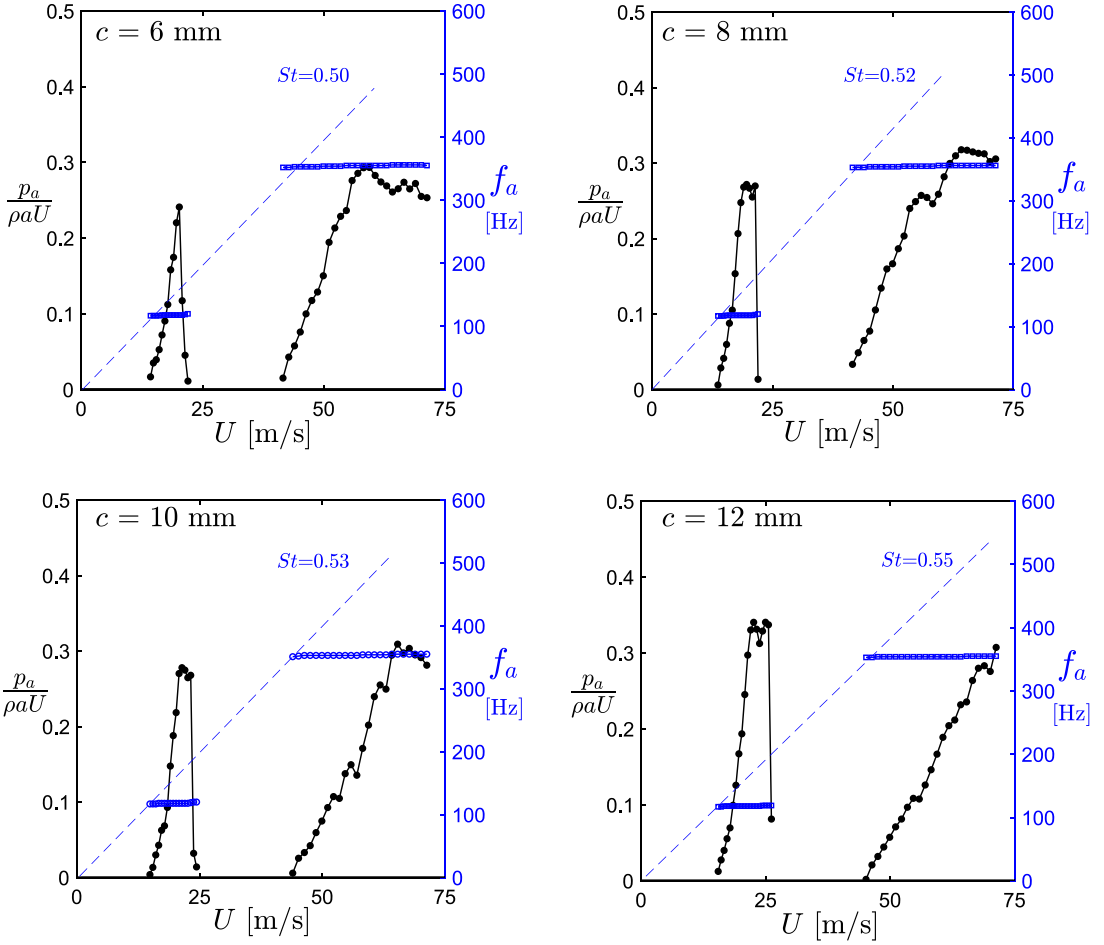


Fig. 11. The aeroacoustic response of coaxial side branches with different chamfered edges .

Table 1
Geometric configurations of cases considered in Fig. 14.

L/λ	l_{up} [m]	L/D
3/4	2.24	22.4
5/4	3.73	37.3
7/4	5.22	52.2
9/4	6.71	67.1

Table 2
Model predictions of the aeroacoustic response for coaxial branches at different upstream distances.

l_{up}	St	Lock-in range	$p_a/\rho aU$
2.24	0.46	St = 0.30–0.46	0.077
3.73	0.53	St = 0.36–0.53	0.103
5.22	0.62	St = 0.39–0.62	0.115
6.71	0.62	St = 0.39–0.62	0.115

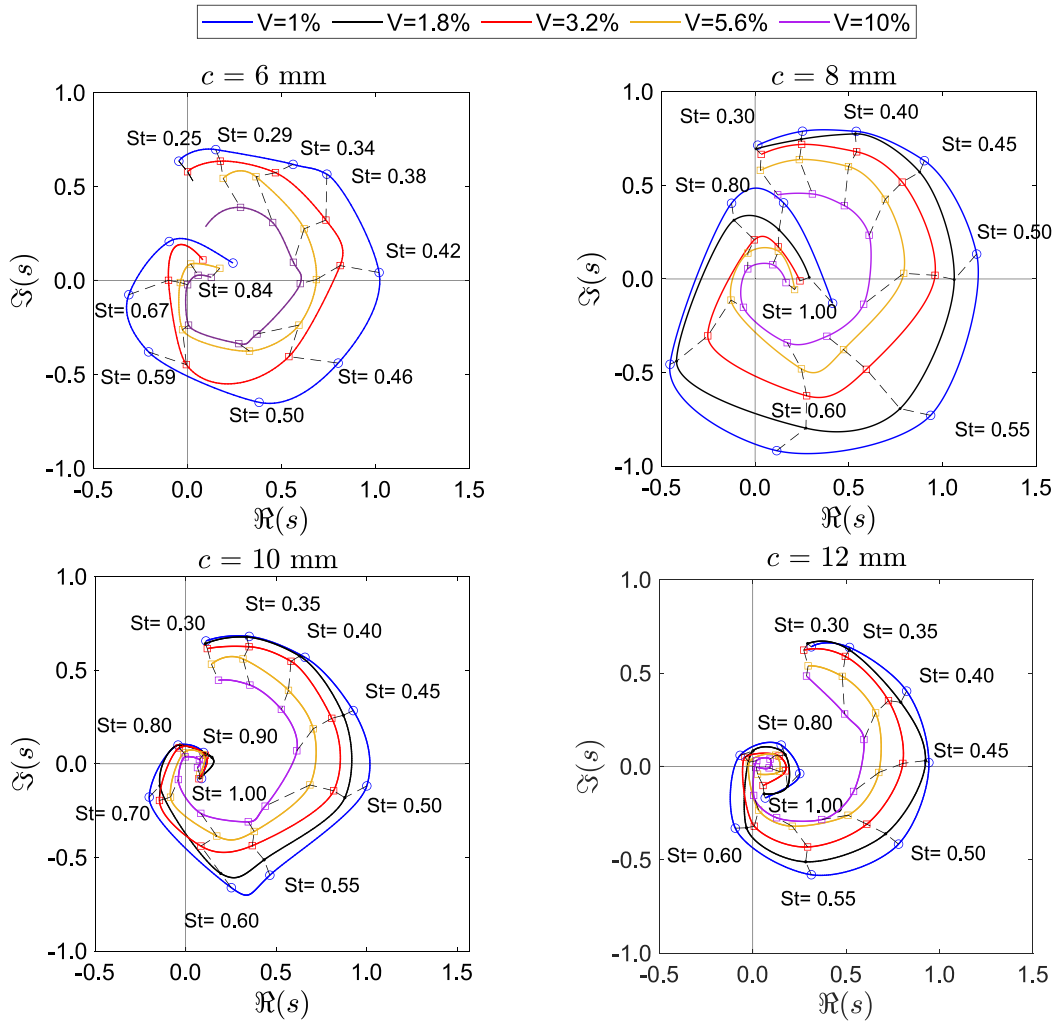


Fig. 12. The aeroacoustic complex sound source maps for coaxial branches of chamfered edges with different chamfering length.

shear layer development. A longer distances are expected to allow for a higher shear layer thickness until the flow is fully developed at the upstream edge.

Using the method discussed before in Section 3, the acoustic resonance parameters determined from the source maps in Fig. 15 are included in Table 2. Increasing the upstream distance resulted in an increase in the Strouhal number at which the peak resonance is expected. For the shortest upstream distance, maximum acoustic pressure is predicted at $St = 0.46$. This increases gradually to 0.62 at $l_{up} = 7\lambda/4$, then becomes constant. The same is true for the three other parameters selected. The Strouhal numbers over which resonance is observed increases slightly such that resonance starts at 0.39 and lasts until 0.62. The normalized acoustic pressure at resonance increases from 0.077 to 0.115. The saturation of these values is likely a result of the full development of the flow, as well as the decrease of the acoustic radiation losses into the main pipe to the extent that these losses become insignificant for the two longest upstream pipes. This has significant implications in practical settings, as it means that the piping branching segments most susceptible for resonance excitation would be present in fully developed flow conditions and away from open ends.

6. Conclusion

In this study, the excitation of acoustic resonance in the configuration of coaxial pipe branches is experimentally investigated. A lumped element model of the shear layer is used to calculate the complex acoustic source representing the contribution of the shear layer perturbation to resonance excitation. Moreover, the source term can be used to predict the acoustic pressure amplitude and frequency of acoustic resonance at prescribed flow conditions. For validation, the model is successfully used to evaluate the susceptibility of a coaxial side branch to acoustic resonance excitation. The predicted acoustic resonance parameters, including

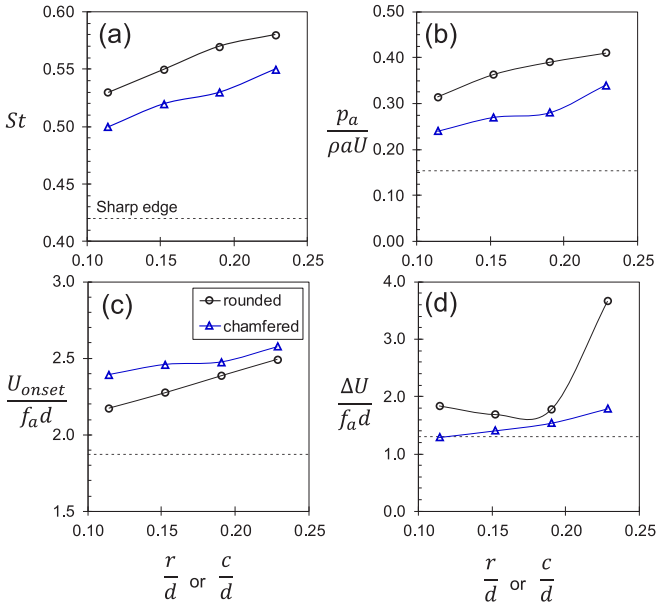


Fig. 13. The effect of normalized junction edge geometry on the acoustic resonance parameters of coaxial branches (a) Strouhal number, (b) normalized acoustic pressure, (c) onset flow velocity, and (d) lock-in flow velocity range.

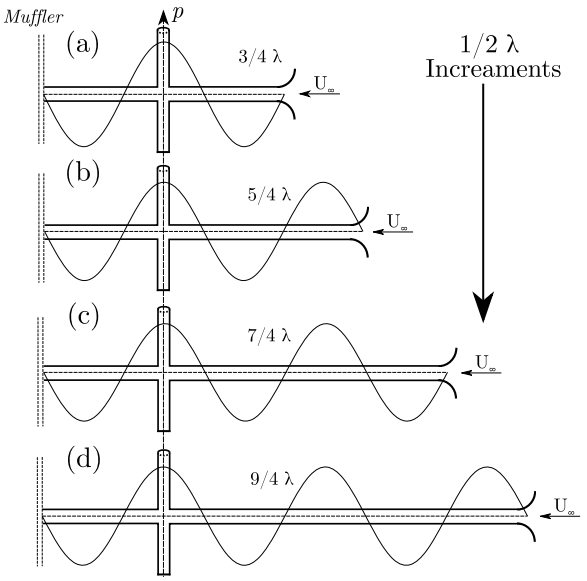


Fig. 14. The tested configurations for varying the upstream distance with decoupled cavity mode for an open–open acoustic boundary condition.

the Strouhal number, the normalized acoustic pressure amplitude over a range of flow velocities agree well with experimental observations

Moreover, the influence of the branching junction edge geometry modifications; namely rounding and chamfering on the parameters of the excited acoustic resonance is explored. Results showed that the edge parameters had a significant effect on several features of the excited acoustic resonance. First, rounding the edges excites resonance of a higher acoustic pressure amplitude than both chamfered and sharp edges. The excitation of resonance occurs at higher Strouhal numbers. Moreover, the increase in rounding radius results in an increase in the onset flow velocity and the flow velocity range over which resonance is observed. These observations show that edge modifications can introduce added risk of acoustic mode excitation by the shear layers.

In addition, the influence of the upstream flow conditions on the excitation of acoustic resonance is experimentally investigated. In four considered configurations, the branching junction is located at different distances from the upstream end at locations where

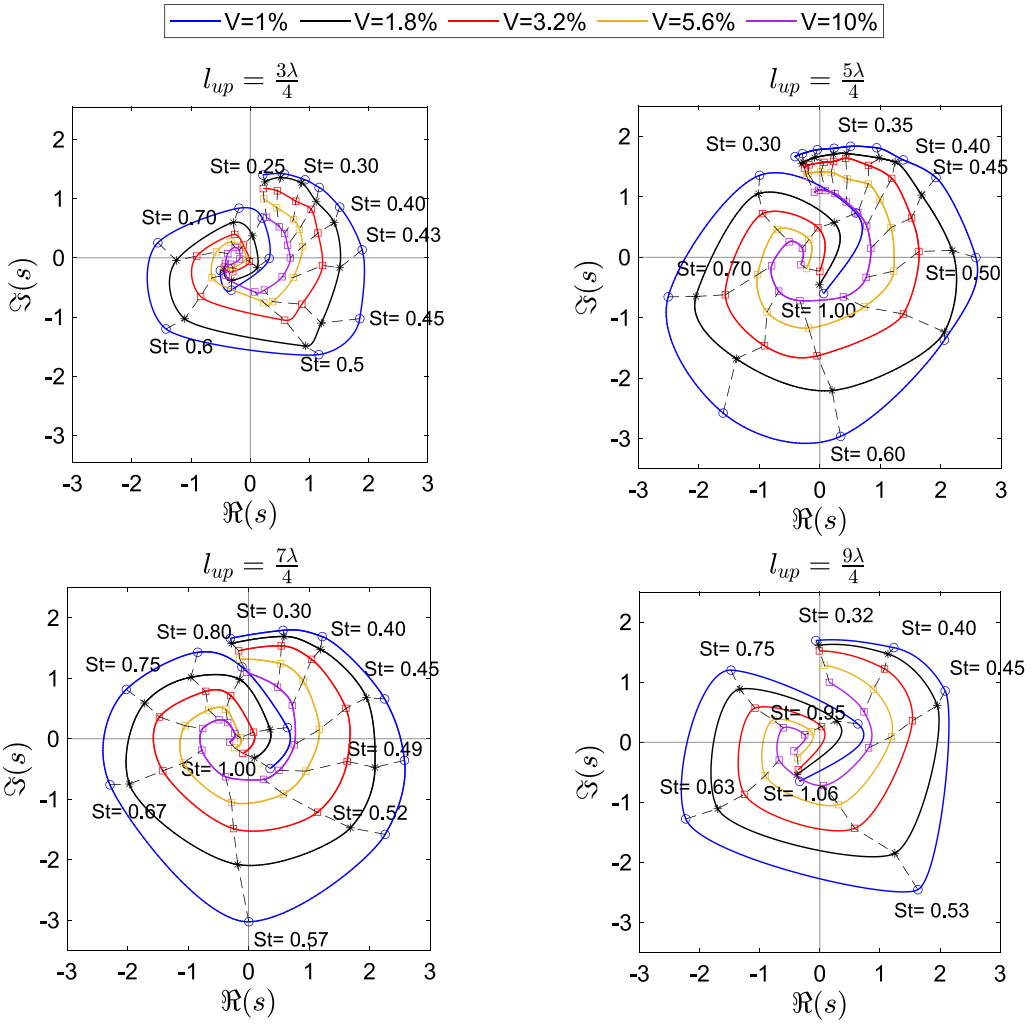


Fig. 15. The aeroacoustic complex sound source for coaxial branches of sharp edges with different distances to the upstream end.

the acoustic impedance at the acoustic mode frequency of the branch is maximized. Results show that junctions at higher distances from the upstream edge are more susceptible to acoustic resonance excitation, and excite resonance at higher Strouhal numbers. However, the predicted acoustic amplitude reaches a maximum level once the upstream distance is sufficient for the flow to be fully developed over the branching junction. This behavior is likely influenced by the thickness of the shear layer, as well as the acoustic radiation losses into the upstream pipe. These results have significant implications in piping systems, as it indicates that the piping branching segments most susceptible for resonance excitation would be present in fully developed flow conditions and away from open ends.

CRediT authorship contribution statement

Atef Mohany: Writing – original draft, Visualization, Supervision, Project administration, Methodology, Funding acquisition, Conceptualization. **Omar Hammad:** Writing – original draft, Validation, Formal analysis, Data curation. **Hossam Kishawy:** Writing – review & editing, Resources. **Marwan Hassan:** Writing – review & editing, Resources. **Mahmoud Shaaban:** Writing – original draft, Methodology, Formal analysis, Conceptualization.

Declaration of competing interest

The authors declare that they have no known competing financial interests or personal relationships that could have appeared to influence the work reported in this paper.

Acknowledgments

The authors thankfully acknowledge the financial support provided by the Natural Sciences and Engineering Research Council of Canada (NSERC).

Data availability

Data will be made available on request.

References

[1] S. Ziada, Flow-excited acoustic resonance in industry, J. Press. Vessel. Technol. 132 (1) (2010) 015001–015009.
[2] S. Ziada, P. Lafon, Flow-excited acoustic resonance excitation mechanism, design guidelines, and counter measures, Appl. Mech. Rev. 66 (1) (2014) 010802.
[3] L. Jiang, H. Zhang, Q. Duan, Y. Zhang, Numerical study on acoustic resonance excitation in closed side branch pipeline conveying natural gas, Shock. Vib. 2020 (1) (2020) 8857838.
[4] M. Shaaban, A. Mohany, Flow–acoustic coupling around rectangular rods of different aspect ratios and incidence angles, Exp. Fluids 63 (2) (2022) 45.
[5] H. Zhang, P. Wang, H. Liu, B. Wang, Y. Liu, Unsteady flow behaviors and flow-induced noise characteristics in a closed branch T-junction, Phys. Fluids 36 (6) (2024).
[6] D.S. Weaver, S. Ziada, M.K. Au-Yang, S.S. Chen, M.P. Paidoussis, M.J. Pettigrew, Flow-induced vibrations in power and process plant components—Progress and prospects , J. Press. Vessel. Technol. 122 (3) (2000) 339–348.
[7] D. Arthurs, S. Ziada, Flow-excited acoustic resonances of coaxial side-branches in an annular duct, J. Fluids Struct. 25 (1) (2009) 42–59.
[8] K. Okuyama, A. Tamura, S. Takahashi, M. Ohtsuka, M. Tsubaki, Flow-induced acoustic resonance at the mouth of one or two side branches, Nucl. Eng. Des. 249 (2012) 154–158.
[9] Y. Xiao, W. Zhao, H. Gu, X. Gao, Effects of branch length and chamfer on flow-induced acoustic resonance in closed side branches, Ann. Nucl. Energy 121 (2018) 186–193.
[10] Y. Xiao, W. Zhang, J. Li, X. Gao, C. Huang, H. Gu, Effects of edge geometry on the flow-induced acoustic resonances in closed side branches, Ann. Nucl. Energy 160 (2021) 108372.
[11] M. Shaaban, A. Mohany, Synchronous vortex shedding from aerodynamically isolated side-by-side cylinders imposed by flow-excited resonant acoustic modes, Exp. Fluids 62 (2021) 1–17.
[12] M. Hanna, A. Mohany, Aeroacoustics and shear layer characteristics of confined cavities subject to low Mach number flow, J. Fluids Struct. 121 (2023) 103949.
[13] P.M. Radavich, A. Selamet, J.M. Novak, A computational approach for flow–acoustic coupling in closed side branches, J. Acoust. Soc. Am. 109 (4) (2001) 1343–1353.
[14] P. Wang, L. He, Y. Liu, Acoustics-driven vortex dynamics in channel branches with round intersections: Flow mode transition and three-dimensionality, Phys. Fluids 32 (2) (2020).
[15] M. Abdelmwgoud, M. Shaaban, A. Mohany, Shear layer synchronization of aerodynamically isolated opposite cavities due to acoustic resonance excitation, Phys. Fluids 33 (5) (2021).
[16] M. Shaaban, R. Noufal, M. Alziadeh, A. Mohany, Spinning dynamics of self-excited azimuthal acoustic modes in cavities, Phys. Fluids 36 (7) (2024).
[17] D. Tonon, J. Willems, A. Hirschberg, Self-sustained oscillations in pipe systems with multiple deep side branches: Prediction and reduction by detuning, J. Sound Vib. 330 (24) (2011) 5894–5912.
[18] M. El Hassan, L. Keirsbulck, L. Labraga, Non-oscillating/oscillating shear layer over a large deep cavity at low-subsonic speeds, Flow Turbul. Combust. 82 (2009) 359–374.
[19] J.L. Wagner, S.J. Beresh, K.M. Casper, E.P. DeMauro, S. Arunajatesan, Resonance dynamics in compressible cavity flows using time-resolved velocity and surface pressure fields, J. Fluid Mech. 830 (2017) 494–527.
[20] S. Ziada, E. Bühlmann, Self-excited resonances of two side-branches in close proximity, J. Fluids Struct. 6 (5) (1992) 583–601.
[21] P. Oshkai, T. Yan, Experimental investigation of coaxial side branch resonators, J. Fluids Struct. 24 (4) (2008) 589–603.
[22] J.C. Bruggeman, A. Hirschberg, M.E.H. van Dongen, A.P.J. Wijnands, J. Gorter, Flow induced pulsations in gas transport systems: Analysis of the influence of closed side branches, J. Fluids Eng. 111 (4) (1989) 484–491.
[23] M.S. Howe, Vortex sound, in: Theory of Vortex Sound, in: Cambridge Texts in Applied Mathematics, Cambridge University Press, 2002, pp. 114–135.
[24] S. Dequand, S. Hulshoff, A. Hirschberg, Self-sustained oscillations in a closed side branch system, J. Sound Vib. 265 (2) (2003) 359–386.
[25] M. Abom, M. Karlsson, A. Kierkegaard, On the use of linear aero-acoustic methods to predict whistling, in: 16th International Congress on Sound and Vibration 2009, ICSV 2009, KTH, Marcus Wallenberg Laboratory MWL, 2009, pp. 2406–2413, Qc 20140923.
[26] M. Karlsson, M. Abom, Aeroacoustics of T-junctions—An experimental investigation, J. Sound Vib. 329 (10) (2010) 1793–1808.
[27] J.C. Bruggeman, A. Hirschberg, M.E. van Dongen, A.P. Wijnands, J. Gorter, Self-sustained aero-acoustic pulsations in gas transport systems: experimental study of the influence of closed side branches, J. Sound Vib. 150 (3) (1991) 371–393.
[28] P. Kriesels, M. Peters, A. Hirschberg, A. Wijnands, A. Iafrati, G. Riccardi, R. Piva, J. Bruggeman, High amplitude vortex-induced pulsations in a gas transport system, J. Sound Vib. 184 (2) (1995) 343–368.
[29] M. Meissner, Flow-excited acoustic pulsations in ducts with closed side branches, Arch. Acoust. 22 (2) (1997) 153–168.
[30] P. Oshkai, T. Yan, A. Velikorodny, S. VanCaeseele, Acoustic power calculation in deep cavity flows: A semiempirical approach, J. Fluids Eng. 130 (5) (2008) 051203.
[31] H.R. Graf, S. Ziada, Excitation source of a side-branch shear layer, J. Sound Vib. 329 (14) (2010) 2825–2842.
[32] J. Doherty, P. Ngan, J. Monty, M. Chong, The development of turbulent pipe flow, in: Proceedings of 16th Australasian Fluid Mechanics Conference, School of Engineering, The University of Queensland, Gold Coast, Australia, 2007.
[33] S. Allam, M. Abom, Investigation of damping and radiation using full plane wave decomposition in ducts, J. Sound Vib. 292 (3–5) (2006) 519–534.
[34] S. Ziada, S. Shine, Strouhal numbers of flow-excited acoustic resonance of closed side branches, J. Fluids Struct. 13 (1) (1999) 127–142.
[35] R. Ma, P.E. Slaboch, S.C. Morris, Fluid mechanics of the flow-excited Helmholtz resonator, J. Fluid Mech. 623 (2009) 1–26.
[36] P.T. Nagy, P. Rucz, A. Szabó, Examination of jet growth and jet-drive in the recorder by means of linearized numerical and lumped models, J. Sound Vib. 527 (2022) 116857.
[37] H. Tijdeman, On the propagation of sound waves in cylindrical tubes, J. Sound Vib. 39 (1) (1975) 1–33.
[38] A. Omer, N. Arafa, A. Mohany, M. Hassan, The effect of upstream edge geometry on the acoustic resonance excitation in shallow rectangular cavities, Int. J. Aeroacoustics 15 (3) (2016) 253–275.